Low Energy Ion Implantation Induced Intermixing in Photonic Devices: Defect Profiling and Evolution

F. Schiettekatte[1], V. Aimez[2], M. Chicoine[1], S. Chevobbe[2], J.F. Chabot[1], J.F. Rajotte[1]

1.Département de Physique, Université de Montréal, Canada
2.Département de Génie Électrique et de Génie Informatique , Université de Sherbrooke, Canada

Abstract. Low energy ion implantation of InP heterostructures has proved to be an efficient way to induce controlled quantum well intermixing. A significant blue-shift, dependent on local ion dose, appears after a 600°C anneal, which is not observed in the unimplanted regions. Thus, this technique makes possible the fabrication of integrated photonic devices working at several wavelengths. However, it has been observed that the shift is also influenced by the implantation temperature: 200°C implants induce much more intermixing than room temperature implants. In this paper, we will establish a relation between the implant temperature, the induced blue-shift and the amount of defects in the implanted region, as measured by channeling-RBS. A much lower defect concentration is observed for higher temperature implants, which implies that a significant number of defects diffuse in-depth during the implantation in order to provide efficient intermixing.

INTRODUCTION

Optical fiber telecommunications are constantly improving, exhibiting a drastic growth in bandwidth. This is namely achieved through faster optoelectronic devices, but also by the development of many optical and photonic devices (e.g. Er-doped fiber amplifier) in order to reduce the amount of electronic components that usually contribute to slow down the overall operation speed of the system. But another technique, wavelength division multiplexing (WDM), developed especially over the last decade, has also contributed to increase the fibers bandwidth by multiplying the number of available channels. Up to now, such multiplexing was generally achieved by combining the signals of different single-wavelength devices. Multiple wavelength integration on a single photonic device would allow a significant improvement of the performance and costs associated with multiplexing. It would also enable a much higher degree of interoperability between the different channels, allowing important developments towards photonic circuits and processing. A problem arises from the difficulty of integrating the components on the same device. Lasers and modulators are based on Quantum Well (QW) structures fabricated by epitaxial growth. As illustrated in Fig. 1, multi-wavelength lasers imply structures with different bandgap values. Electro-optic modulators require semi-absorbing regions for quantum confined Stark effect. Integration of low absorption waveguides also involves even higher bandgap structures. Currently, in order to fabricate these structures, techniques such as selective area epitaxy and etching and regrowth are used.[1] But these methods require several cycles of epitaxial growth in order to create the different components, meaning high costs and limited throughput. An attractive alternative is to use Quantum Well Intermixing (QWI).[2] By controllably inducing an inter-diffusion at QW interfaces, the shape of the well is smoothed and its wavelength blue-shifted.

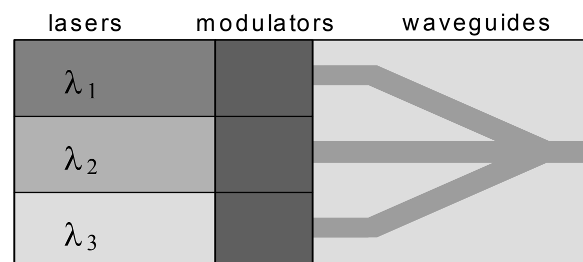

FIGURE 1. Schematic representation of an integrated photonic device. Each laser has a different wavelength; the modulator bandgaps have to be adjusted so that they are semi-absorbing at their laser wavelength; the waveguide bandgap must be high enough to achieve low absorption.

QWI by Low Energy Implantation

Intermixing can be achieved locally and reliably by low energy ion implantation.[3] Defects are created near the surface, and then diffused through the QW structure. At a given energy, the amount of intermixing depends on the dose and ion species. Selected areas of a device can thus be implanted at specific doses in order to provide the amount of blue-shift required by the different components of an integrated photonic device. Considering that low energy implanters are available in most fabrication facilities, and that selective area implantation only relies on photolithography, QWI by low energy implantation can be a cost-effective method for preparing such devices.

In the case of InP-based QW, low energy ion implantations are typically carried out with 200-400 keV P or As. A maximum of ~100 nm blue-shift is obtained for doses of the order of 1×10^{14} at/cm^2 and implantation temperatures of 200°C, followed by a 650°C annealing. Contrarily to high-energy implantation (directly in or through the QW), which induces a lot of damage to the QW structure and drastically impairs its performance, low energy implantation does not contribute to decrease the quality of the device.[3] Secondary defects can be found in the implantation zone after annealing, but they are located near the surface, far away from the active region. A detailed review on the effects of dose, ion energy and substrate temperature on the characteristics of photonic integrated devices can be found in Ref. 4. In most of these reports, however, the evaluation of the quantity of implantation damage and its distribution relies on TRIM simulations.[5] Meanwhile, effects such as damage accumulation or dynamic annealing at elevated implantation temperatures can hardly be taken into account. The relation between the amount of damage and the blue-shift is thus not directly established experimentally.

In order to understand the fundamentals of the process, gaining information on the actual defect distribution after implantation and its relation with implantation temperature is of prime importance. This can then allow the development of strategies to overcome some limitations of the techniques (e.g. in terms of maximum blue-shift achievable and reproducibility). Initial measurements of defect profiles after implantation by means of Rutherford Backscattering Spectrometry (RBS) in channeling mode are presented here. Comparison between the defect profile obtained after Room Temperature (RT) and 200°C implantations are reported. They are compared to the photoluminescence (PL) for these samples and results obtained form other experiments.

EXPERIMENTAL

A lattice-matched QW structure has been grown on a (100) InP sulfur-doped substrate by Chemical Beam Epitaxy (CBE) at NRC in Ottawa. It consists of a single InGaAs 5 nm QW in between two 20 nm quaternary barriers (q=1.3). The structure is completed by 4 additional layers, a 30 nm InP layer, a 10 nm quaternary etch stop (q=1.3), a 1.4 μm upper cladding InP Layer and a top 150 nm InGaAs contact layer. The heterostructures have been implanted either by phosphorus, arsenic or xenon ions with fixed energies of 200 or 360 keV, with doses ranging from 5×10^{12} to 2×10^{14} at/cm^2. Implantations have been carried out on the 200 kV Varian DF-3000 implanter of the Université de Sherbrooke and on the 1.7 MV Tandetron accelerator of the Université de Montréal. The implanted structures were annealed in a Rapid Thermal Annealing furnace at either 650°C or 700°C during 120s. The defect profiles were obtained from RBS-channeling measurements on the Tandetron accelerator using either 2 or 3 MeV He^+ beam. The channeling direction was found with a precision better than 0.1° by interpolating between planar channeling directions.

RESULTS AND DISCUSSION

Defect Profiles

200 keV As implantations were carried out in the InGaAs contact layer. The ions actually reach the InP capping layer. As seen in Fig. 2, an important amount of damage is generated in the sample for RT implantations (up to 13% of displaced atoms). This distribution also shows two maxima. One is located near the half of the InGaAs layer and corresponds to the damage peak for such implantation in InGaAs (60 nm), while a second maximum is observed at the InGaAs/InP interface (150 nm).

In Fig. 2b), the measured defect profile (thick solid line) is compared to SRIM 2000 simulations. For both simulations, a fairly high displacement energy of E_d = 20 eV was used for the InGaAs but, even though, the predicted amount of damage at 60 nm is about twice the value found experimentally. On the other hand, a uniform displacement energy of 20 eV for all atoms (InGaAs and InP layers) returns a relatively smooth profile (thin solid line) and only shows a tiny peak at the interface, due to the larger In concentration in InP compared to InGaAs. A displacement energy of only 4

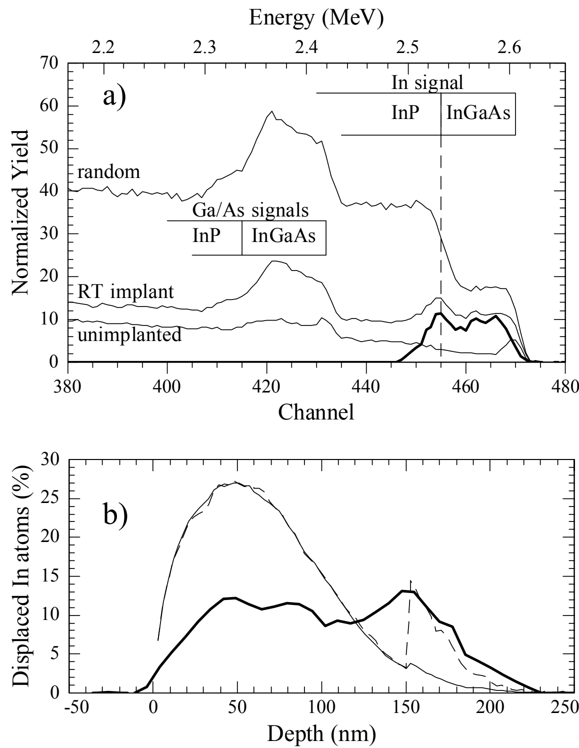

FIGURE 2. a) RBS-channeling spectra for InGaAs/InP implanted with 1×10^{14} As/cm^2 at 200 keV at RT. The thick line represents the net damage contribution distribution to the RT spectrum; b) actual damage depth profile (thick solid line) compared to recoiled In atoms as calculated by SRIM simulations with an InP displacement energy of 20 eV (thin solid line) and 4 eV (thin dashed line).

eV has to be set for the atoms of the InP layer in order to approach the experimental data. (Here, we have to consider the fact that the experimental defect profile is broadened by depth resolution.) Consequently, it appears that the relative amount of damage created in the InP is much higher than it is in the InGaAs contact layer.

This can also be seen from Fig. 3a), where the InGaAs contact layer has been etched out selectively prior to implantation. Similar doses of As where implanted, but this time the sample is heavily damaged, as the channeling signal reaches that of a randomly oriented target. This stresses out the fact that InP is much more sensitive to ion-induced damage than InGaAs.

It is also seen from Fig. 3a) that the "amorphized" layer is thinner in the case of the 200°C implants. Therefore, an important dynamical annealing process appears to occur during such implantations. This effect is also strong in InGaAs as it is also responsible for the absence of detectable damage in the sample of Fig. 3b) implanted at higher temperature. Similar conclusions can also be drawn form 360 keV Xe^{++} implantations into the InGaAs contact layer (not shown here) where the damage of the 200°C is spread over a shallower depth than for RT implants. Another feature of Fig. 3b) is that while no damage profile can be extracted from the implantation region, the amount of dechanneling at lower energies increases with dose. This reflects the presence of residual damage either in the implantation region or deeper in the sample.

These results emphasize that defect profiles are highly influenced by the type of material and temperature. Direct defect measurements are required in order to correctly determine the amount and type of damage and effects such as dynamic annealing.

Relationship with Photoluminescence

The PL spectra have been measured for the different samples (Fig. 4). The results are summarized in Table 1 in terms of PL blue-shift after a 700°C anneal for 120 s. As evidenced by earlier work,[3,4] the maximum amount of shift is obtained for 200°C implants. It is also seen that no shift is observed for heavily damaged samples.

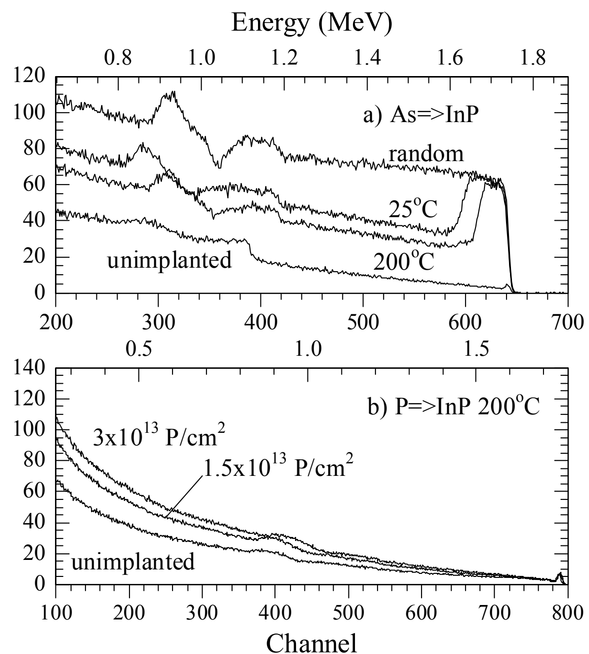

FIGURE 3. a) RBS-channeling spectra for 1×10^{14} As/cm^2 implanted at 200 keV directly in the InP (InGaAs cap layer removed), both at RT and 200°C. b) spectra for 200 keV P implanted in InP at 200°C.

TABLE 1. Summary of damage and PL shift.

Implant	Damage	PL shift (nm)
RT, InGaAs/InP	13%	17
200°C, InGaAs/InP	no obs. Damage	99
RT, InP	Heavy damage	no shift
200°C, InP	Heavy damage	no shift

Thus, an inverse correlation between the amount of damage and blue-shift arises from these results. Obviously, as RBS-channeling is sensitive only to a relatively large amount of damage, at this time we can tell only indirectly (i.e. from the dechanneling) what happens below its sensitivity threshold. But it becomes clear that any important accumulation of damage will worsen the process. However, in order to increase the amount of blue-shift, the most direct way would be to increase the number of point defects involved in the intermixing, which usually implies higher implantation doses.

On the one hand, if stronger blue-shifts are obtained from higher implant temperatures where diffusion must be faster, it also suggests that in these conditions the defects may reach deeper depths *during* the implantation. On the other hand, during RT implantations, damage accumulation favors the formation of trapping sites for the defects like point defect complexes. In order for them to diffuse and induce blue-shift, the defects must be in a state in which they are easily released at annealing time, and low temperature implantation or easily damageable material such as InP both contribute to reduce the number of mobile point defects.

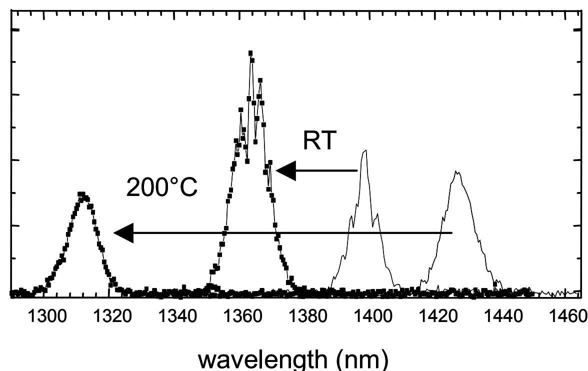

FIGURE 4. PL shift obtained after an implantation of 1×10^{14} As/cm^2 at RT and 200°C followed by a 700°C anneal for 120 seconds. At this annealing temperature, an unimplanted sample would shift by ~13 nm due to thermally induced intermixing. (Initial peaks are not at the same wavelength mainly because of QW non-uniformity across the wafer.)

CONCLUSION

Quantum Well Intermixing has proved to be a powerful technique in order to fabricate Photonic Integrated Devices. However, information is required on the actual amount of damage create during the implantation (rather than the one obtained by simulation) in order to correlate it with the amount of blue-shift observed. In this paper, we showed that reduced performances of the technique in the case of relatively high dose implantations seem to be associated with the accumulation of damage. It is also suggested that better shifts are obtained at elevated temperatures because the ion-induced damage diffuses in depth prior to the annealing and the defects are thus less susceptible of being trapped or to form clusters than at RT.

Acknowledgments

The authors are grateful to Réal Gosselin, Louis Godbout and P. Lafrance for their technical assistance, as well as P. Poole from NRC for sample CBE growth. This work benefited of grants from the NSERC of Canada and FCAR of Québec.

REFERENCES

1. E. S. Koteles, “Techniques for Monolithically fabricating Photonic Integrated Circuits,” in *Application of Photonics Technology,* edited by G.A. Lampropoulos, J. Chrostowski, and R.M. Measures, New York: Plenum, 1997, pp. 413-418, 1995.

2. J. H. Marsh, *Semiconductor Sci. Technol.* **8**, 1136–1155 (1993).

3. V. Aimez, J. Beauvais, J. Beerens, D. Morris, H.S. Lim, B.S. Ooi, J. Selected Topics in Quantum Electronics, 8, 4 (2002).

4. S. Charbonneau, E.S. Koteles, P.J. Poole, J.J. He, G.C. Aers, H. Haysom, M. Buchanan, Y. Feng, A. Delage, F.Yang, M. Davies, R.D. Goldberg, P.G. Piva, and I.V. Mitchell, *J. Select. Topics Quant. Electron.* **4**, 772-793 (1998).

5. J. F. Ziegler, J. P. Biersack, and U. Littmark, *The Stopping and Ion Range of Ions in Matter*, New York : Pergamon, 1985.